nature neuroscience

Article

https://doi.org/10.1038/s41593-022-01174-7

Mendelian randomization analyses support causal relationships between brain imaging-derived phenotypes and risk of psychiatric disorders

Received: 5 February 2021

Accepted: 29 August 2022

Published online: 10 October 2022

Check for updates

Jing Guo[1,3], Ke Yu[1,3], Shan-Shan Dong[1,3], Shi Yao[2], Yu Rong[1], Hao Wu[1], Kun Zhang[1], Feng Jiang[1], Yi-Xiao Chen[2], Yan Guo[1] ✉ and Tie-Lin Yang[1] ✉

Observational studies have reported the correlations between brain imaging-derived phenotypes (IDPs) and psychiatric disorders; however, whether the relationships are causal is uncertain. We conducted bidirectional two-sample Mendelian randomization (MR) analyses to explore the causalities between 587 reliable IDPs (N = 33,224 individuals) and 10 psychiatric disorders (N = 9,725 to 161,405). We identified nine IDPs for which there was evidence of a causal influence on risk of schizophrenia, anorexia nervosa and bipolar disorder. For example, 1 s.d. increase in the orientation dispersion index of the forceps major was associated with 32% lower odds of schizophrenia risk. Reverse MR indicated that only genetically predicted schizophrenia was positively associated with two IDPs, the cortical surface area and the volume of the right pars orbitalis. We established the BrainMR database (http://www.bigc.online/BrainMR/) to share our results. Our findings provide potential strategies for the prediction and intervention for psychiatric disorder risk at the brain-imaging level.

Psychiatric disorders are a group of serious illnesses that result in brain dysfunctions in which individuals are disturbed emotionally, cognitively or behaviorally. Millions of people worldwide have been reported to suffer from psychiatric disorders, which are considered serious public health problems[1,2].

Psychiatric disorders can be characterized by a collection of physiological brain changes, including many heritable imaging-derived phenotypes (IDPs) that can be measured non-invasively using magnetic resonance imaging[3]. A large number of observational case–control studies have been performed to explore the relationships between IDPs and psychiatric disorders. For example, the smaller thicknesses of the insula and rostral anterior cingulate cortex are regarded as cerebral markers for adolescent anxiety[4]. The thicknesses of the temporal and parietal cortex are decreased in individuals with schizophrenia[5] but are increased in individuals with autism spectrum disorder compared to those in healthy individuals[6]. Individuals with bipolar disorder showed lower fractional anisotropy (FA)[7] and greater mean diffusivity (MD)[8] in the posterior thalamic radiation than healthy individuals. Reduced hippocampal volume is found in adolescents with anorexia nervosa[9], elderly individuals with depression[10] and twin pairs with severe post-traumatic stress disorder[11]. There is evidence that thalamic volume is decreased in attention deficit hyperactivity disorder[12] and increased

[1]Key Laboratory of Biomedical Information Engineering of Ministry of Education, Biomedical Informatics & Genomics Center, School of Life Science and Technology, Xi'an Jiaotong University, Xi'an, P. R. China. [2]National and Local Joint Engineering Research Center of Biodiagnosis and Biotherapy, The Second Affiliated Hospital, Xi'an Jiaotong University, Xi'an, P. R. China. [3]These authors contributed equally: Jing Guo, Ke Yu, Shan-Shan Dong. ✉e-mail: guoyan253@xjtu.edu.cn; yangtielin@xjtu.edu.cn

in Tourette syndrome[13]. The brain structural alterations of individuals with obsessive–compulsive disorder are mostly characterized by a reduced cortical surface area in several regions[14]. Although growing evidence suggests that alterations in brain IDPs are associated with psychiatric disorders, the causal link between IDPs and psychiatric disorders remains unclear. Moreover, findings from conventional observational studies could not account for confounding factors. It is critical to explore the putative causal role of IDPs on psychiatric disorders and vice versa.

Mendelian randomization (MR) is a widely used epidemiological method that uses genetic variants as instruments to infer the causality between exposure and outcome[15]. Large-scale genome-wide association studies (GWASs)[16] provide the opportunity to systematically explore the potential causal relationships between numerous IDPs and psychiatric disorders through MR. Therefore, in this study, we performed bidirectional two-sample MR analyses to estimate the causal associations between 587 IDPs and 10 psychiatric disorders (attention deficit hyperactivity disorder, anorexia nervosa, anxiety disorder, autism spectrum disorder, bipolar disorder, major depressive disorder, obsessive–compulsive disorder, posttraumatic stress disorder, schizophrenia and Tourette syndrome). We eventually identified 11 putative causal associations. Furthermore, we established a database called BrainMR (http://www.bigc.online/BrainMR/) to provide a useful resource to share our results. Our findings could offer a perspective to guide the early-stage prevention, etiological diagnosis and treatment of psychiatric disorders at the brain-imaging level.

Results

Overview of the study

The study design is shown in Fig. 1. Referring to previous studies[17–21], we selected 587 reliably measured IDPs (Supplementary Table 1), including the measurements distributed in cerebral cortex, subcortical regions and white matter tracts, from a sample size of up to 33,224 UK Biobank participants. GWAS summary data with sample sizes ranging from 9,725 to 161,405 for 10 psychiatric disorders were collected (Supplementary Table 2). We examined genetic correlations between 587 IDPs and 10 psychiatric disorders before MR analyses and found that 557 IDP–disorder pairs were estimated with nominal P values of <0.05 (Supplementary Table 3 and Supplementary Fig. 1). We conducted bidirectional two-sample MR analysis to investigate the relationships between these IDP–disorder pairs. To make sure that the samples of the exposures were independent from those of the outcomes, we manually checked the sample description of each GWAS study. Except for anorexia nervosa, there was no sample overlap between the data of the IDPs and the other nine psychiatric disorders. For anorexia nervosa[22], the sample overlap proportion was 5%. According to the study by Burgess et al.[23], the bias estimated from a 5% sample overlap was <0.15% in the MR study. Therefore, our MR estimates would not be affected by sample overlap between exposures and outcomes. To adjust for multiple testing, we conducted the Bonferroni correction across all MR tests, including the forward direction and reverse direction after quality control. The significant P value threshold was therefore set as 4.49×10^{-5} (0.05/557/2; 557 denotes the number of IDP–disorder pairs selected by genetic correlation analysis, and two denotes both forward and reverse MR tests).

Instrument variant (IV) selection

After linkage disequilibrium (LD) pruning, we removed the IVs associated with potential confounders (Supplementary Tables 4 and 5). Outlier IVs (Supplementary Tables 6 and 7) were also removed for subsequent MR analysis (Methods). The full lists of IVs used for forward and reverse MR tests are provided in Supplementary Tables 8 and 9. We calculated the F-statistics to assess instrument strength. For the 539 forward and 533 reverse MR pairs with at least one IV, the F-statistic values were all ≥30 (Supplementary Tables 8 and 9), suggesting that these single nucleotide polymorphisms (SNPs) are suitable IVs. We also calculated the statistical power based on the sample size for the MR test[24] (Methods). The results showed that we had 80% power at a significance level of 0.05 to detect a minimum odds ratio (OR) of >1.04 or <0.96 in forward MR analyses (Supplementary Table 8) and a minimum β of >0.07 or <−0.07 in reverse MR analyses (Supplementary Table 9). The power for significance level after multiple testing correction (4.49×10^{-5}) is also provided in Supplementary Tables 8 and 9.

Forward MR of IDPs on psychiatric disorders

As shown in Supplementary Table 10, in forward MR analyses, we identified nine statistically significant causal relationships between nine IDPs in five brain structural categories and three psychiatric disorders, including schizophrenia, anorexia nervosa and bipolar disorder (Fig. 2). The scatter plots of genetic associations with psychiatric disorders over genetic associations with IDPs are shown in Supplementary Fig. 2.

The putative causal effects of IDPs on schizophrenia. As shown in Fig. 2 and Supplementary Table 10, we observed that five IDPs located in four brain structures (the forceps major, tapetum, superior fronto-occipital fasciculus and third ventricle) were causally associated with schizophrenia.

The forceps major is a commissural fiber that connects the occipital cortex of the two cerebral hemispheres via the splenium of the corpus callosum. In this region, 1 s.d. increase in the orientation dispersion index (OD) of the forceps major was associated with 32% lower odds of schizophrenia risk (inverse variance-weighted (IVW) OR = 0.68, 95% confidence interval (95% CI) of 0.61 to 0.78, $P = 2.14 \times 10^{-9}$). OD is used to characterize the angular variation of neurites[25].

The tapetum is a commissural fiber through the splenium of the corpus callosum but connects the inferior temporal lobes on both sides of the cerebral hemisphere. An increase of 1 s.d. in the MD of the tapetum was associated with 35% higher risk of schizophrenia (IVW OR = 1.35, 95% CI of 1.17 to 1.54, $P = 1.89 \times 10^{-5}$). MD is an indicator of the water diffusion in all directions to assess the structural integrity of the brain[26].

The superior fronto-occipital fasciculus is an association fiber connecting the superior frontal lobe and superior parietal lobe[27]. We observed that the FA values of the superior fronto-occipital fasciculus in both brain hemispheres were negatively associated with schizophrenia risk. FA is a measure widely used to evaluate white matter integrity[26]. The risk of schizophrenia increased by 21% per 1 s.d. decrease in FA in the superior fronto-occipital fasciculus of the right hemisphere (IVW OR = 0.79, 95% CI of 0.71 to 0.88, $P = 1.03 \times 10^{-5}$) and by 23% for the same structural alterations in the left hemisphere (IVW OR = 0.77, 95% CI of 0.69 to 0.87, $P = 1.33 \times 10^{-5}$).

The third ventricle is located in the midline of both cerebral hemispheres and consists of the central part of the ventricular system of the brain. An increase of 1 s.d. in volume of the third ventricle was associated with 16% higher risk of schizophrenia (IVW OR = 1.16, 95% CI of 1.08 to 1.24, $P = 2.70 \times 10^{-5}$).

The putative causal effects of IDPs on anorexia nervosa. As shown in Fig. 2 and Supplementary Table 10, we observed that three IDPs located in the superior corona radiata were causally associated with anorexia nervosa. The superior corona radiata is a projection fiber that interconnects with the parietal part of the cerebral cortex and the brain stem through the internal capsule. An increase of 1 s.d. in the MD value of the superior corona radiata in the left hemisphere was associated with 26% higher odds of anorexia nervosa (IVW OR = 1.26, 95% CI of 1.14 to 1.41, $P = 1.79 \times 10^{-5}$). In addition, 1 s.d. increase in the intracellular volume fraction (ICVF) value of the superior corona radiata in the right hemisphere was associated with 18% lower odds of anorexia nervosa (IVW OR = 0.82, 95% CI of 0.75 to 0.90, $P = 1.86 \times 10^{-5}$). Similar structural

https://doi.org/10.1038/s41593-022-01174-7

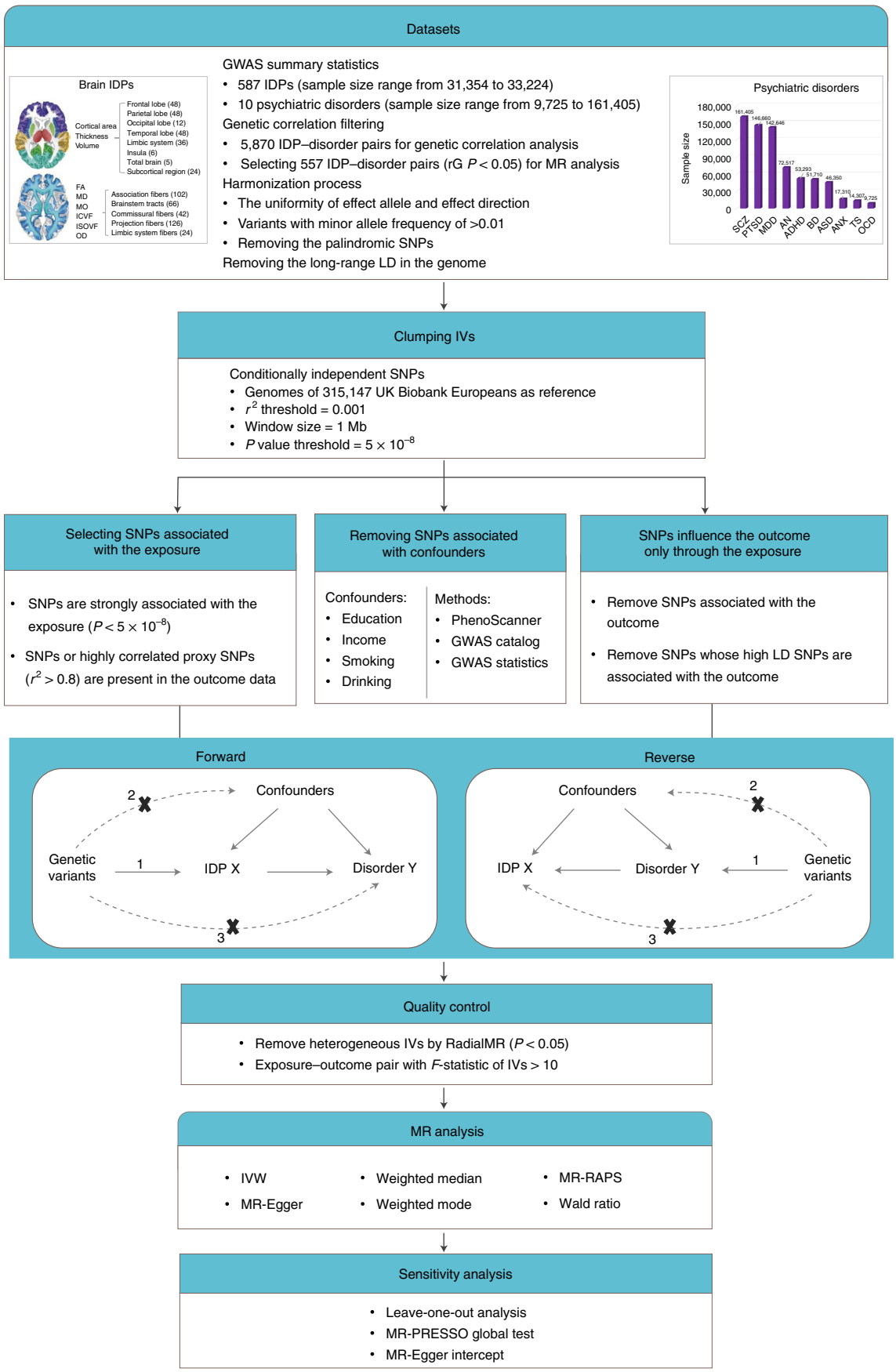

Fig. 1 | Workflow of the causal inference between IDPs and psychiatric disorders. Abbreviations: MO, diffusion tensor mode; ISOVF, isotropic or free water volume fraction; ADHD, attention deficit hyperactivity disorder; ANX, anxiety disorder; ASD, autism spectrum disorder; MDD, major depressive disorder; OCD, obsessive–compulsive disorder; PTSD, posttraumatic stress disorder; TS, Tourette syndrome; rG, genetic correlation.

https://doi.org/10.1038/s41593-022-01174-7

Table 1 | Summary of the literature on bidirectional MR findings

MR results from the current study		Information from previous observational studies		
Exposure	**Outcome (MR + or –)**	**Ref.**	**Cohort**	**Conclusion**
OD in the forceps major	SCZ (–)	Schoorl et al.[30]	768 individuals with a reported history of any psychotic-like experiences, 435 individuals with reported visual psychotic-like experiences	Individuals with reported history of visual psychotic-like experiences had reduced FA of the forceps major
		Sui et al.[31]	47 individuals with SCZ, 50 matched healthy individuals	Individuals with SCZ showed higher FA values of the forceps major
		Friedman et al.[32]	40 individuals with first-episode SCZ and 39 healthy individuals; 40 individuals with chronic SCZ and 40 healthy individuals	Individuals with SCZ showed decreased FA values of the forceps major
FA in the right superior fronto-occipital fasciculus	SCZ (–)	Wang et al.[33]	37 individuals with first-episode SCZ with auditory verbal hallucination, 60 individuals with SCZ without auditory verbal hallucination and 50 healthy individuals	Individuals with SCZ with auditory verbal hallucination showed decreased FA in the right superior fronto-occipital fasciculus
FA in the left superior fronto-occipital fasciculus	SCZ (–)	Wang et al.[34]	126 individuals with SCZ, 99 individuals at genetic high risk for SCZ and 130 healthy individuals	Individuals with SCZ showed decreased FA in the left superior fronto-occipital fasciculus
MD in the left tapetum	SCZ (+)	Lu et al.[8]	21 individuals with SCZ and 18 healthy individuals	Individuals with SCZ showed a greater MD in the tapetum
Volume of the third ventricle	SCZ (+)	de Zwarte et al.[35]	1,228 first-degree relatives of individuals with SCZ, 1,016 individuals with SCZ and 2,246 healthy individuals	Individuals with SCZ showed larger volume of the third ventricle
		Brugger et al.[36]	3,901 individuals with first-episode SCZ and 4,040 healthy individuals	
MD in the left superior corona radiata	AN (+)	Miles et al.[37]	23 underweight women with AN, 23 weight-recovered women with AN and 24 healthy individuals	Women with acute and remitted AN showed greater MD in the corona radiata
ICVF in the right superior corona radiata	AN (–)	Frank et al.[38]	19 adolescents with AN and 22 healthy individuals	Adolescents or women with AN showed reduced FA values of the superior corona radiata
		Frieling et al.[39]	21 women with AN and 20 healthy individuals	
ICVF in the left superior corona radiata		Vogel et al.[40]	22 adolescent females with AN and 21 healthy individuals	
Volume of the left accumbens	BD (–)	Ohi et al.[41]	51 individuals with BD and 205 healthy controls	The volume of the left accumbens was reduced in individuals with BD
		Dickstein et al.[42]	20 children with BD and 20 matched healthy individuals	
		Rimol et al.[5]	139 individuals with BD and 207 healthy individuals	Individuals with BD showed reduced substantial subcortical volume in the right nucleus accumbens
SCZ	Cortical surface area of the right pars orbitalis (+)	Nenadic et al.[43]	87 individuals with SCZ and 108 healthy individuals	Individuals with SCZ showed an increased fractal dimension in the right pars orbitalis, which reflects cortical surface abnormalities
SCZ	Volume of the right pars orbitalis (+)	Francis et al.[44]	46 young adults at high familial risk of SCZ and 31 healthy individuals with no family history of illness	Individuals with high familial risk of SCZ showed smaller volume of left pars triangularis

The notations '+' and '–' refer to positive and negative associations detected by MR analyses. Abbreviations: SCZ, schizophrenia; AN, anorexia nervosa; BD, bipolar disorder.

changes in the left hemisphere were also associated with a lower risk of anorexia nervosa (IVW OR = 0.82, 95% CI of 0.75 to 0.90, $P = 3.15 \times 10^{-5}$). ICVF is a meaningful microstructural parameter for measuring neurite density based on intracellular diffusion[25].

The putative causal effects of IDPs on bipolar disorder. As shown in Fig. 2 and Supplementary Table 10, we observed that one IDP located in the accumbens of the left hemispheric subcortical region was negatively associated with bipolar disorder. The accumbens is a region between the basal forebrain and the hypothalamus and plays a key role in action selection, integrating cognitive and affective information[28]. An increase of 1 s.d. in the volume of the left accumbens was associated with 46% lower risk of bipolar disorder (IVW OR = 0.54, 95% CI of 0.40 to 0.73, $P = 4.47 \times 10^{-5}$).

Reverse MR of psychiatric disorders on IDPs

We did not detect significant causal effects of psychiatric disorders on the nine IDPs detected by the forward MR analyses in the reverse MR analyses (Supplementary Table 11). However, we found evidence that schizophrenia was positively associated with another two IDPs (Fig. 3). Both IDPs were derived from measurements of the pars orbitalis in the right hemisphere, which is located in the frontal lobe of the cortex. Higher risk of schizophrenia was associated with increased cortical surface area (IVW $\beta = 0.06$, 95% CI of 0.04 to 0.08, $P = 1.24 \times 10^{-7}$) and

https://doi.org/10.1038/s41593-022-01174-7

Exposure (ID)	IDP category	Outcome	IVs *N*	Method	OR (95% CI)	*P* value
OD in the forceps major (IDP.2035)	Commissural fiber	SCZ	6	IVW	0.68 (0.61 to 0.78)	2.14×10^{-9}
				MR-RAPS	0.68 (0.59 to 0.79)	1.04×10^{-7}
				Weight median	0.68 (0.59 to 0.80)	2.06×10^{-6}
				Weight mode	0.65 (0.49 to 0.86)	1.11×10^{-2}
				MR-Egger	0.59 (0.34 to 1.02)	5.41×10^{-2}
FA in the right superior fronto -occipital fasciculus (IDP.1494)	Association fiber	SCZ	8	IVW	0.79 (0.71 to 0.88)	1.03×10^{-5}
				MR-RAPS	0.79 (0.70 to 0.88)	3.24×10^{-5}
				Weight median	0.78 (0.68 to 0.90)	5.24×10^{-4}
				Weight mode	0.77 (0.60 to 0.99)	4.34×10^{-2}
				MR-Egger	0.47 (0.21 to 1.04)	5.80×10^{-2}
FA in the left superior fronto -occipital fasciculus (IDP.1495)	Association fiber	SCZ	9	IVW	0.77 (0.69 to 0.87)	1.33×10^{-5}
				MR-RAPS	0.76 (0.67 to 0.86)	5.98×10^{-6}
				Weight median	0.75 (0.65 to 0.87)	1.16×10^{-4}
				Weight mode	0.71 (0.56 to 0.91)	1.24×10^{-2}
				MR-Egger	0.35 (0.15 to 0.82)	2.22×10^{-2}
MD in the left tapetum (IDP.1649)	Commissural fiber	SCZ	6	IVW	1.35 (1.17 to 1.54)	1.89×10^{-5}
				MR-RAPS	1.35 (1.16 to 1.57)	1.28×10^{-4}
				Weight median	1.33 (1.12 to 1.58)	1.07×10^{-3}
				Weight mode	1.32 (1.01 to 1.72)	4.54×10^{-2}
				MR-Egger	1.50 (0.40 to 5.65)	4.40×10^{-1}
Volume of the third ventricle (IDP.0174)	Subcortical region	SCZ	16	IVW	1.16 (1.08 to 1.24)	2.70×10^{-5}
				MR-RAPS	1.16 (1.08 to 1.25)	5.49×10^{-5}
				Weight median	1.17 (1.06 to 1.28)	1.31×10^{-3}
				Weight mode	1.17 (1.00 to 1.36)	4.85×10^{-2}
				MR-Egger	1.12 (0.78 to 1.60)	5.24×10^{-1}
MD in the left superior corona radiata (IDP.1627)	Projection fiber	AN	20	IVW	1.26 (1.14 to 1.41)	1.79×10^{-5}
				MR-RAPS	1.27 (1.13 to 1.42)	4.91×10^{-5}
				Weight median	1.23 (1.05 to 1.45)	9.51×10^{-3}
				Weight mode	1.23 (0.98 to 1.54)	7.12×10^{-2}
				MR-Egger	1.25 (0.86 to 1.83)	2.25×10^{-1}
ICVF in the right superior corona radiata (IDP.1926)	Projection fiber	AN	25	IVW	0.82 (0.75 to 0.90)	1.86×10^{-5}
				MR-RAPS	0.82 (0.75 to 0.91)	5.87×10^{-5}
				Weight median	0.86 (0.76 to 0.99)	3.26×10^{-2}
				Weight mode	0.85 (0.71 to 1.03)	9.56×10^{-2}
				MR-Egger	0.79 (0.61 to 1.04)	8.92×10^{-2}
ICVF in the left superior corona radiata (IDP.1927)	Projection fiber	AN	24	IVW	0.82 (0.75 to 0.90)	3.15×10^{-5}
				MR-RAPS	0.82 (0.75 to 0.90)	6.09×10^{-5}
				Weight median	0.86 (0.75 to 0.99)	3.34×10^{-2}
				Weight mode	0.84 (0.70 to 1.01)	6.30×10^{-2}
				MR-Egger	0.86 (0.65 to 1.14)	2.73×10^{-1}
Volume of the left accumbens (IDP.0023)	Subcortical region	BD	4	IVW	0.54 (0.40 to 0.73)	4.47×10^{-5}
				MR-RAPS	0.54 (0.38 to 0.75)	2.21×10^{-4}
				Weight median	0.52 (0.36 to 0.76)	5.69×10^{-4}
				Weight mode	0.84 (0.70 to 1.01)	6.30×10^{-2}
				MR-Egger	0.10 (0.00 to 3,203)	4.36×10^{-1}

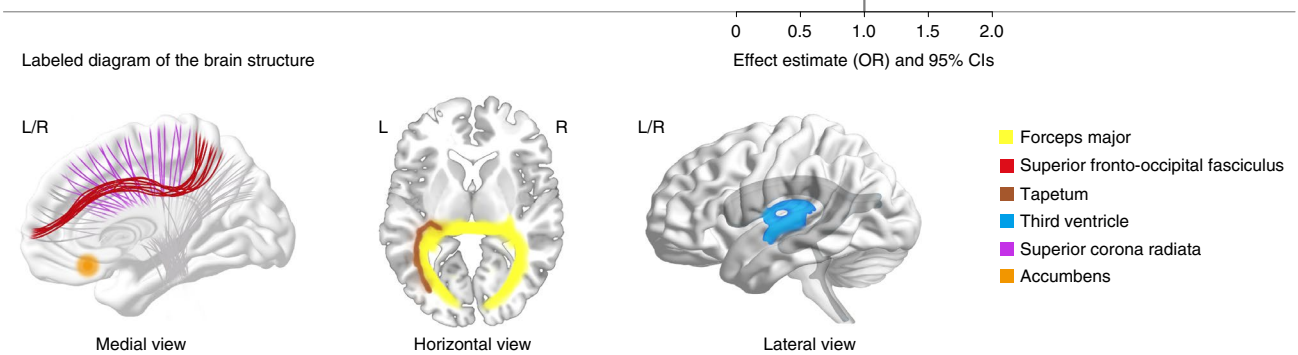

Fig. 2 | Causalities in the forward MR. The forest plot shows the significant causalities. The effect estimates represent the log (OR) of disorder per 1 s.d. change in mean IDP, and the error bars represent 95% CIs. All statistical tests were two sided. $P < 4.49 \times 10^{-5}$ after Bonferroni correction was considered significant. Arrows indicate that the maximum interval on the *x* axis is extended. The pattern diagram in the bottom shows the brain anatomical region of the corresponding IDP; L, left; R, right. Causal effects were estimated using five two-sample MR methods (IVW, MR-RAPS, weighted median, weighted mode and MR-Egger).

https://doi.org/10.1038/s41593-022-01174-7

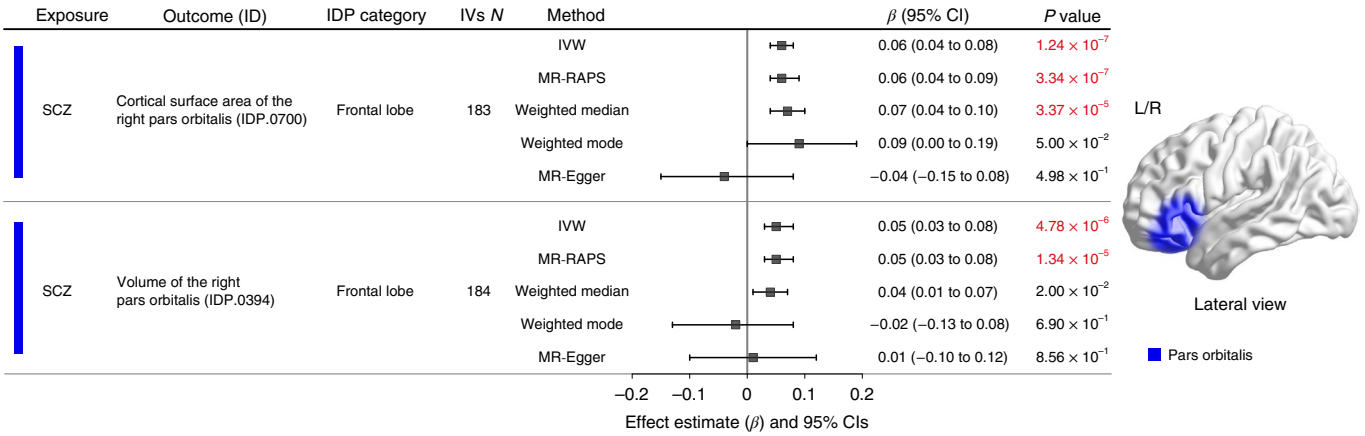

Fig. 3 | Causalities in the reverse MR. The forest plot shows the significant causalities. The effect estimates represent change in mean IDP per unit change in disorder, and the error bars represent 95% CI. All statistical tests were two sided. A P value of $<4.49 \times 10^{-5}$ after Bonferroni correction was considered significant. The pattern diagram on the right shows the brain anatomical region of the corresponding IDP. Causal effects were estimated using five two-sample MR methods (IVW, MR-RAPS, weighted median, weighted mode and MR-Egger).

volume (IVW $\beta = 0.05$, 95% CI of 0.03 to 0.08, $P = 4.78 \times 10^{-6}$) of the right pars orbitalis.

Sensitivity analyses

We performed sensitivity analyses to verify our putative causalities obtained with bidirectional MR. First, leave-one-out analyses showed that no single SNP drove the causal estimates (Supplementary Figs. 2 and 3). Second, the global MR pleiotropy residual sum and outlier (MR-PRESSO) test did not detect any evidence of horizontal pleiotropy (Supplementary Tables 12 and 13). Third, MR-Egger intercepts of all associations were close to zero, suggesting that no significant pleiotropy was detected (Supplementary Tables 12 and 13). Fourth, the directions of the estimates from the other four MR methods were the same as those of the IVW method. However, using the same threshold ($P < 4.49 \times 10^{-5}$), the numbers of associations supported by the MR robust adjusted profile score (MR-RAPS), weighted median, weighted mode and MR-Egger method were only 5, 2, 0 and 0, respectively (Figs. 2 and 3). The difference may be due to the fact that the power of these four methods is smaller than that of the IVW[29]. Overall, the sensitivity analyses confirmed the reliability of our putative causal effects in both the forward and reverse MR results.

Additionally, we performed test–retest correlation to evaluate the reliability for the IDPs that showed significant MR signals in our study. The results showed that the test–retest correlation values for the IDPs with significant MR signals were all >0.70 (Supplementary Table 14), supporting the reliability of the IDP data. To check whether there was unintended bias arising from the confounders filtering procedure, we also compared the IVW results before and after confounder filtering (Supplementary Table 15). The results showed that the MR estimates after confounder filtering were generally similar but had wider CIs than those without filtering. However, after multiple testing corrections, the significant IDP–disorder pairs remained the same between the two groups.

Interpretation of the putative causalities

According to the previously published evidence in the literature, we summarized the biological insights or clinical observational studies for causality results of bidirectional MR in Table 1 (refs. [5,8,30–44]).

Specifically, for schizophrenia, the five IDPs detected in the forward MR analyses were different from the two IDPs detected in the reverse MR analyses. In addition, the five IDPs were not genetically correlated with the two IDPs (Supplementary Fig. 4). All of our results were integrated into an open online BrainMR database (http://www.bigc.online/BrainMR/) for public access.

Discussion

Observational studies have reported that IDPs are associated with psychiatric disorders; however, whether the relationships are causal is uncertain. In the present study, we performed bidirectional two-sample MR analyses to systematically investigate the causal associations between 587 IDPs and 10 psychiatric disorders. We identified nine IDPs where there was evidence of a causal influence on schizophrenia, anorexia nervosa and bipolar disorder. Moreover, we identified potential causal effects of schizophrenia on two IDPs.

Schizophrenia is a complex and severe psychiatric disorder that is associated with multiple factors. In the forward MR analysis, we found that IDPs in the forceps major, tapetum, superior fronto-occipital fasciculus and third ventricle were associated with schizophrenia. The forceps major is a commissural fiber involved in the pathway connecting the hippocampal complex to visual regions. We observed a negative association between the OD of the forceps major and schizophrenia. OD is a neurite orientation dispersion and density imaging-derived metric that reflects variations in neurite fiber orientations[25]. The reduced OD is likely to imply a reduction in the complexity of dendrites and axons[25]. Although evidence from observational studies between OD of the forceps major and schizophrenia is lacking, FA of the forceps major has been reported to be decreased[32] or increased[31] in individuals with schizophrenia. Similar to the forceps major, the tapetum is a commissural fiber. We detected an adverse effect of increased MD value of the left tapetum on schizophrenia. Consistently, a previous observational study reported that individuals with schizophrenia showed greater MD in the tapetum than healthy individuals[8].

The superior fronto-occipital fasciculus is an association fiber that originates from the superior frontal gyrus and terminates in the superior parietal lobe, which has the potential functions of visual processing and spatial consciousness[45]. We discovered that the FA values in the superior fronto-occipital fasciculus from both hemispheres were negatively correlated with the risk of schizophrenia. A previous case–control study of schizophrenia showed identical differences in the superior fronto-occipital fasciculus[46]. Moreover, individuals with schizophrenia with auditory verbal hallucination showed decreased FA in the right superior fronto-occipital fasciculus[33]. Considering that individuals with schizophrenia exhibit visual/auditory processing impairments, our findings may be useful for future research in this aspect.

The enlarged volume of the third ventricle was observed as a potential risk factor for schizophrenia in our analysis. Consistently, several observational studies reported that the volume of the third ventricle in individuals with schizophrenia was larger than that in healthy individuals[35,36]. Enlarged ventricles, such as the lateral and third ventricles, in individuals with schizophrenia are closely associated with atrophy of brain structures such as the thalamus, striatum and insula[47]. The main cause of ventricular dilatation is due to an imbalance in cerebrospinal fluid circulation, which leads to excessive accumulation of cerebrospinal fluid and ultimately disrupts the development and function of the human cerebral cortex[48].

Trubetskoy et al. found that genetic enrichments for schizophrenia showed the strongest overlaps with neuronal but not glial cell types[49]. Consistently, the IDPs identified in our forward MR analysis (for example FA, MD, OD and ICVF in white matter structures) are widely used to evaluate the variation of neurites and reflect the properties of axons. Moreover, the two IDPs we identified from reverse MR are located in the gray matter, where neuronal cell bodies are usually located. We observed putative causal effects of schizophrenia on the cortical area and the volume of the right pars orbitalis. The pars orbitalis is part of the inferior frontal gyrus, which has been shown to be involved in language and comprehension functions of the brain[50]. Similar to our results, a previous study showed significant alterations of cortical surface area of the right pars orbitalis in individuals with schizophrenia[43]. However, the relationship between the volume of the right pars orbitalis and schizophrenia from a previous observational study[44] is inconsistent. Because observational studies are unable to fully account for confounding factors, our results may offer help to clarify the association between surface area of the pars orbitalis and schizophrenia.

Anorexia nervosa is a life-threatening eating disorder and a psychiatric condition characterized by inaccurate perception and persistent energy restriction, which leads to severely low body weight[51]. The IDPs associated with anorexia nervosa are located in the superior corona radiata region. The superior corona radiata is one of the key structures of signal transmission and carries both ascending and descending nerve signals between the corticospinal tract and cerebral cortex. Specifically, our results showed that an increase in MD values in the left superior corona radiata and a decrease in ICVF values in the bilateral superior corona radiata were associated with anorexia nervosa. Consistently, a previous study suggested that women with acute and remitted anorexia nervosa showed greater MD in the corona radiata than healthy individuals[37]. Lesions of the corona radiata and internal capsule have been found to cause alterations or disturbances in taste and smell[52]. Unfortunately, to date, no relevant studies have been conducted on the measurement of ICVF in the superior corona radiata. By contrast, a decrease in FA value of the superior corona radiata has been widely reported in adolescents or women with anorexia nervosa[38–40]. ICVF is a neurite orientation dispersion and density imaging-derived metric that reflects neurite density[25]. The decrease in FA may be caused by a decrease in neuronal density[25]. Therefore, our findings implied that ICVF measures are potential markers that may be used in the future for etiology research and diagnosis.

Bipolar disorder is a serious psychiatric condition that causes extreme mood swings, including feelings of extreme euphoria or extreme depression[53]. In our study, we observed that the volume of the left accumbens was negatively associated with bipolar disorder. Consistently, several observational studies[5,41,42] also showed that the volume of the accumbens was reduced in individuals with bipolar disorder. Abnormalities in the nucleus accumbens are critical to the pathophysiology of reward deficits in mood-related behaviors[54]. However, there is also observational evidence showing that the volume of the left accumbens is increased[55] or unchanged[56] in individuals with bipolar disorder. Our results may offer help to clarify this inconsistency.

Our study provides a comprehensive investigation to identify causal relationships between 587 reliable IDPs and 10 psychiatric disorders. MR results may be different from the observational case–control findings. This is likely due to the fact that the case versus control evidence may be the result of medications or environment/lifestyle changes, whereas the MR findings are not. MR uses genetic polymorphisms as a proxy for exposure to infer a causal relationship between exposure and outcome. Because genetic IVs are randomly distributed in the population, the results of MR are robust to the impact of confounding factors[15]. In addition, to keep our results robust, we used conservative Bonferroni corrections for multiple testing. Under such circumstances, some previously reported significant causal relationships may not remain in our study. For example, a previous study by Shen et al.[57] discovered the potential causal effects of major depressive disorder on four IDPs (MD in the thalamic radiations, ICVF in the superior longitudinal fasciculus, ICVF in the forceps major and MD in the total white matter tracts), which were not found in our study. This might be affected by several factors. First, compared to their IDPs, the IDPs we used were subdivided into the left and right hemispheres and the directional anatomical regions (anterior, posterior, superior and inferior). Second, the GWAS data of IDPs and major depressive disorder were different to some extent. Although we used their IVs to conduct the MR analysis, the results were not significant after multiple testing corrections.

The limitations of our study should be addressed. First, because the IDP summary data are from the UK Biobank, we have tried our best to avoid sample overlap by selecting psychiatric data without the UK Biobank sample. However, for anorexia nervosa, there was a 5% overlap with the UK Biobank sample[22]. We could not exclude these samples due to the lack of detailed information on these overlapping participants. Second, populations of different ethnicities have different LD structures and allele frequencies, and using the data from complicated ethnic backgrounds may lead to weak instrument variants and a potential bias in causal estimates[58]. The summary data we used here were from the publicly available GWAS database; therefore, we were unable to assess the impact of population stratification on our results. The samples of selected data in our study were of European ancestry, except for schizophrenia[49], where approximately 80% of the individuals in the data were of European origin and the rest were of East Asian origin. Third, because the GWAS data of different psychiatric disorders had different powers due to the limitation of sample sizes, the cross-sectional comparisons at IDP levels could not be performed. In addition, the estimated MR effect size must be treated cautiously when applied to clinical interventions. The desirable application of predictive results to clinical and health care decisions depends on the effect size of the exposure on the outcome. However, MR uses exposure risk SNPs to study the effects of lifetime exposure factors on outcomes rather than a specific intervention over a period of time[59]. Therefore, the effect size of the results of our MR analysis should not be considered equivalent to the effect size of randomized controlled trials for short-term interventions.

In conclusion, we conducted bidirectional two-sample MR analyses to systematically estimate the underlying causal relationships between neuroimaging phenotypes and psychiatric disorders using large-scale GWAS data. The findings revealed strong genetic evidence for causal links between neuroimaging phenotypes and psychiatric disorders. This will contribute to better prediction and intervention at the brain-imaging level for potential risk of psychiatric disorders.

Online content

Any methods, additional references, Nature Research reporting summaries, source data, extended data, supplementary information, acknowledgements, peer review information; details of author contributions and competing interests; and statements of data and code availability are available at https://doi.org/10.1038/s41593-022-01174-7.

References

1. Charlson, F. et al. New WHO prevalence estimates of mental disorders in conflict settings: a systematic review and meta-analysis. *Lancet* **394**, 240–248 (2019).
2. Disease, G. B. D., Injury, I. & Prevalence, C. Global, regional, and national incidence, prevalence, and years lived with disability for 354 diseases and injuries for 195 countries and territories, 1990–2017: a systematic analysis for the Global Burden of Disease Study 2017. *Lancet* **392**, 1789–1858 (2018).
3. Miller, K. L. et al. Multimodal population brain imaging in the UK Biobank prospective epidemiological study. *Nat. Neurosci.* **19**, 1523–1536 (2016).
4. Suffren, S., Chauret, M., Nassim, M., Lepore, F. & Maheu, F. S. On a continuum to anxiety disorders: adolescents at parental risk for anxiety show smaller rostral anterior cingulate cortex and insula thickness. *J. Affect. Disord.* **248**, 34–41 (2019).
5. Rimol, L. M. et al. Cortical thickness and subcortical volumes in schizophrenia and bipolar disorder. *Biol. Psychiatry* **68**, 41–50 (2010).
6. Hardan, A. Y., Muddasani, S., Vemulapalli, M., Keshavan, M. S. & Minshew, N. J. An MRI study of increased cortical thickness in autism. *Am. J. Psychiatry* **163**, 1290–1292 (2006).
7. Saricicek, A. et al. Abnormal white matter integrity as a structural endophenotype for bipolar disorder. *Psychol. Med.* **46**, 1547–1558 (2016).
8. Lu, L. H., Zhou, X. J., Keedy, S. K., Reilly, J. L. & Sweeney, J. A. White matter microstructure in untreated first episode bipolar disorder with psychosis: comparison with schizophrenia. *Bipolar Disord.* **13**, 604–613 (2011).
9. King, J. A. et al. Global cortical thinning in acute anorexia nervosa normalizes following long-term weight restoration. *Biol. Psychiatry* **77**, 624–632 (2015).
10. Ballmaier, M. et al. Hippocampal morphology and distinguishing late-onset from early-onset elderly depression. *Am. J. Psychiatry* **165**, 229–237 (2008).
11. Gilbertson, M. W. et al. Smaller hippocampal volume predicts pathologic vulnerability to psychological trauma. *Nat. Neurosci.* **5**, 1242–1247 (2002).
12. Seidman, L. J. et al. Gray matter alterations in adults with attention-deficit/hyperactivity disorder identified by voxel based morphometry. *Biol. Psychiatry* **69**, 857–866 (2011).
13. Greene, D. J. et al. Brain structure in pediatric Tourette syndrome. *Mol. Psychiatry* **22**, 972–980 (2017).
14. Rus, O. G. et al. Structural alterations in patients with obsessive–compulsive disorder: a surface-based analysis of cortical volume, surface area and thickness. *J. Psychiatry Neurosci.* **42**, 395–403 (2017).
15. Davey Smith, G. & Hemani, G. Mendelian randomization: genetic anchors for causal inference in epidemiological studies. *Hum. Mol. Genet.* **23**, R89–R98 (2014).
16. Smith, S. M. et al. An expanded set of genome-wide association studies of brain imaging phenotypes in UK Biobank. *Nat. Neurosci.* **24**, 737–745 (2021).
17. Iscan, Z. et al. Test–retest reliability of freesurfer measurements within and between sites: effects of visual approval process. *Hum. Brain Mapp.* **36**, 3472–3485 (2015).
18. Nugent, A. C. et al. Automated subcortical segmentation using FIRST: test–retest reliability, interscanner reliability, and comparison to manual segmentation. *Hum. Brain Mapp.* **34**, 2313–2329 (2013).
19. Fischl, B. et al. Whole brain segmentation: automated labeling of neuroanatomical structures in the human brain. *Neuron* **33**, 341–355 (2002).
20. Smith, S. M. et al. Tract-based spatial statistics: voxelwise analysis of multi-subject diffusion data. *NeuroImage* **31**, 1487–1505 (2006).
21. Behrens, T. E., Berg, H. J., Jbabdi, S., Rushworth, M. F. & Woolrich, M. W. Probabilistic diffusion tractography with multiple fibre orientations: what can we gain. *NeuroImage* **34**, 144–155 (2007).
22. Watson, H. J. et al. Genome-wide association study identifies eight risk loci and implicates metabo-psychiatric origins for anorexia nervosa. *Nat. Genet.* **51**, 1207–1214 (2019).
23. Burgess, S., Davies, N. M. & Thompson, S. G. Bias due to participant overlap in two-sample Mendelian randomization. *Genet. Epidemiol.* **40**, 597–608 (2016).
24. Burgess, S. Sample size and power calculations in Mendelian randomization with a single instrumental variable and a binary outcome. *Int. J. Epidemiol.* **43**, 922–929 (2014).
25. Zhang, H., Schneider, T., Wheeler-Kingshott, C. A. & Alexander, D. C. NODDI: practical in vivo neurite orientation dispersion and density imaging of the human brain. *NeuroImage* **61**, 1000–1016 (2012).
26. Alexander, A. L., Lee, J. E., Lazar, M. & Field, A. S. Diffusion tensor imaging of the brain. *Neurotherapeutics* **4**, 316–329 (2007).
27. Bao, Y., Wang, Y., Wang, W. & Wang, Y. The superior fronto-occipital fasciculus in the human brain revealed by diffusion spectrum imaging tractography: an anatomical reality or a methodological artifact. *Front. Neuroanat.* **11**, 119 (2017).
28. Floresco, S. B. The nucleus accumbens: an interface between cognition, emotion, and action. *Annu. Rev. Psychol.* **66**, 25–52 (2015).
29. Hartwig, F. P., Davey Smith, G. & Bowden, J. Robust inference in summary data Mendelian randomization via the zero modal pleiotropy assumption. *Int. J. Epidemiol.* **46**, 1985–1998 (2017).
30. Schoorl, J. et al. Grey and white matter associations of psychotic-like experiences in a general population sample (UK Biobank). *Transl. Psychiatry* **11**, 21 (2021).
31. Sui, J. et al. In search of multimodal neuroimaging biomarkers of cognitive deficits in schizophrenia. *Biol. Psychiatry* **78**, 794–804 (2015).
32. Friedman, J. I. et al. Diffusion tensor imaging findings in first-episode and chronic schizophrenia patients. *Am. J. Psychiatry* **165**, 1024–1032 (2008).
33. Wang, Z. et al. The integrity of the white matter in first-episode schizophrenia patients with auditory verbal hallucinations: an atlas-based DTI analysis. *Psychiatry Res. Neuroimaging* **315**, 111328 (2021).
34. Wang, Y. et al. Altered structural connectivity and cytokine levels in schizophrenia and genetic high-risk individuals: associations with disease states and vulnerability. *Schizophr. Res.* **223**, 158–165 (2020).
35. de Zwarte, S. M. C. et al. The association between familial risk and brain abnormalities is disease specific: an ENIGMA-Relatives study of schizophrenia and bipolar disorder. *Biol. Psychiatry* **86**, 545–556 (2019).
36. Brugger, S. P. & Howes, O. D. Heterogeneity and homogeneity of regional brain structure in schizophrenia: a meta-analysis. *JAMA Psychiatry* **74**, 1104–1111 (2017).
37. Miles, A. E., Kaplan, A. S., French, L. & Voineskos, A. N. White matter microstructure in women with acute and remitted anorexia nervosa: an exploratory neuroimaging study. *Brain Imaging Behav.* **14**, 2429–2437 (2020).
38. Frank, G. K., Shott, M. E., Hagman, J. O. & Yang, T. T. Localized brain volume and white matter integrity alterations in adolescent anorexia nervosa. *J. Am. Acad. Child Adolesc. Psychiatry* **52**, 1066–1075 e1065 (2013).
39. Frieling, H. et al. Microstructural abnormalities of the posterior thalamic radiation and the mediodorsal thalamic nuclei in females with anorexia nervosa—a voxel based diffusion tensor imaging (DTI) study. *J. Psychiatr. Res.* **46**, 1237–1242 (2012).

40. Vogel, K. et al. White matter microstructural changes in adolescent anorexia nervosa including an exploratory longitudinal study. *NeuroImage Clin.* **11**, 614–621 (2016).
41. Ohi, K. et al. Differences in subcortical brain volumes among patients with schizophrenia and bipolar disorder and healthy controls. *J. Psychiatry Neurosci.* **47**, E77–E85 (2022).
42. Dickstein, D. P. et al. Frontotemporal alterations in pediatric bipolar disorder: results of a voxel-based morphometry study. *Arch. Gen. Psychiatry* **62**, 734–741 (2005).
43. Nenadic, I., Yotter, R. A., Sauer, H. & Gaser, C. Cortical surface complexity in frontal and temporal areas varies across subgroups of schizophrenia. *Hum. Brain Mapp.* **35**, 1691–1699 (2014).
44. Francis, A. N. et al. Alterations in brain structures underlying language function in young adults at high familial risk for schizophrenia. *Schizophr. Res.* **141**, 65–71 (2012).
45. Forkel, S. J. et al. The anatomy of fronto-occipital connections from early blunt dissections to contemporary tractography. *Cortex* **56**, 73–84 (2014).
46. Kelly, S. et al. Widespread white matter microstructural differences in schizophrenia across 4322 individuals: results from the ENIGMA Schizophrenia DTI Working Group. *Mol. Psychiatry* **23**, 1261–1269 (2018).
47. Gaser, C., Nenadic, I., Buchsbaum, B. R., Hazlett, E. A. & Buchsbaum, M. S. Ventricular enlargement in schizophrenia related to volume reduction of the thalamus, striatum, and superior temporal cortex. *Am. J. Psychiatry* **161**, 154–156 (2004).
48. Duy, P. Q. et al. Brain ventricles as windows into brain development and disease. *Neuron* **110**, 12–15 (2022).
49. Trubetskoy, V. et al. Mapping genomic loci implicates genes and synaptic biology in schizophrenia. *Nature* **604**, 502–508 (2022).
50. Pulvermuller, F. & Fadiga, L. Active perception: sensorimotor circuits as a cortical basis for language. *Nat. Rev. Neurosci.* **11**, 351–360 (2010).
51. Treasure, J. et al. Anorexia nervosa. *Nat. Rev. Dis. Prim.* **1**, 15074 (2015).
52. Onoda, K., Ikeda, M., Sekine, H. & Ogawa, H. Clinical study of central taste disorders and discussion of the central gustatory pathway. *J. Neurol.* **259**, 261–266 (2012).
53. McIntyre, R. S. et al. Bipolar disorders. *Lancet* **396**, 1841–1856 (2020).
54. Sharma, A. et al. Common dimensional reward deficits across mood and psychotic disorders: a connectome-wide association study. *Am. J. Psychiatry* **174**, 657–666 (2017).
55. Ahn, M. S. et al. Anatomic brain magnetic resonance imaging of the basal ganglia in pediatric bipolar disorder. *J. Affect Disord.* **104**, 147–154 (2007).
56. Hibar, D. P. et al. Subcortical volumetric abnormalities in bipolar disorder. *Mol. Psychiatry* **21**, 1710–1716 (2016).
57. Shen, X. et al. A phenome-wide association and Mendelian Rrandomisation study of polygenic risk for depression in UK Biobank. *Nat. Commun.* **11**, 2301 (2020).
58. Pierce, B. L. & Burgess, S. Efficient design for Mendelian randomization studies: subsample and 2-sample instrumental variable estimators. *Am. J. Epidemiol.* **178**, 1177–1184 (2013).
59. Davies, N. M., Holmes, M. V. & Davey Smith, G. Reading Mendelian randomisation studies: a guide, glossary, and checklist for clinicians. *Brit. Med. J.* **362**, k601 (2018).

Methods

Ethics declarations

This research was approved by the ethics committee of Xi'an Jiaotong University. We used the brain-imaging data under UK Biobank application 46387, with T.-L.Y. as principal investigator. The UK Biobank received ethical approval from the North West Multi-Centre Research Ethics Committee. Other publicly available GWAS data have their own ethical approvals; please see the respective references.

Datasets

Brain IDPs. We used the GWAS summary statistics of IDPs processed by Smith et al.[16] with a sample size of 33,224 individuals of European ancestry from the UK Biobank, release 2020. Based on reliable segmentation and meaningful measurement[17–21], 587 brain structural IDPs were selected from the 3,913 original releases, including 203 IDPs in the cerebral cortex, 24 IDPs in subcortical regions and 360 IDPs of white matter connections. We further classified these IDPs into 13 regional categories and 9 measures (Fig. 1). The tools or analyses used to get these measurements are reliable and are described.

1. Cortical measurements were extracted by the FreeSurfer tool based on the Desikan–Killiany atlas[17].
2. Subcortical measurements were extracted by the FIRST tool[18] and the FreeSurfer tool based on the automatic subcortical segmentation[19].
3. The features of white matter connections were estimated from the diffusion magnetic resonance imaging based on two complementary analyses, tract-based spatial statistics[20] and probabilistic tractography[21].

Details of these neuroimaging measures and processing methods[60] are provided by the online reference of UK Biobank (https://biobank.ctsu.ox.ac.uk/crystal/crystal/docs/brain_mri.pdf). All GWAS summary statistics on IDPs were obtained from the Oxford Brain Imaging Genetics (BIG40) web browser (https://open.win.ox.ac.uk/ukbiobank/big40/)[16]. Detailed data information is summarized in Supplementary Table 1.

Psychiatric disorders. We collected 10 psychiatric disorders with publicly available GWAS summary statistics, including attention deficit hyperactivity disorder[61], anorexia nervosa[22], anxiety[62], autism spectrum disorder[63], bipolar disorder[64], major depressive disorder[65], obsessive–compulsive disorder[66], posttraumatic stress disorder[67], schizophrenia[49] and Tourette syndrome[68]. Most of these data were derived from the Psychiatric Genomics Consortium (https://www.med.unc.edu/pgc/download-results), except for posttraumatic stress disorder symptoms in the US Million Veteran Program[67]. The sample sizes for these 10 disorders ranged from 9,725 to 161,405 individuals. Except for anorexia nervosa, all studies had no overlapping individuals from the UK Biobank. Anorexia nervosa had a 5% overlap with the UK Biobank sample; that is, among the 16,992 individuals with anorexia nervosa and 55,525 healthy individuals, 768 individuals with anorexia nervosa and 3,065 healthy individuals were from the UK Biobank[22]. This small percentage of sample overlap was not sufficient to bias the MR study[23]. The samples of psychiatric data selected in our study were largely of European ancestry. The detailed information is summarized in Supplementary Table 2 and the Supplementary Note.

Harmonization of the datasets. We removed variants with minor allele frequencies of <0.01 in the GWAS datasets. For the case–control GWAS summary statistics, the OR was converted to log odds. We removed the palindromic SNPs with minor allele frequencies close to 0.5 following the pipeline in the TwoSampleMR v0.4.26 R package (https://mrcieu.github.io/TwoSampleMR/)[69]. These palindromic SNPs (for example, their alleles are A/T or G/C) would introduce potential strand flipping issues and lead to ambiguity into the harmonization of the effect allele between the exposure and outcome datasets[70]. We defined the minor alleles as effect alleles and ensured that the variants in the exposure and outcome datasets were consistent and all came from the same directional DNA strand. We removed SNPs within long LD regions[71] in the genome from GWAS summary data (https://genome.sph.umich.edu/wiki/Regions_of_high_linkage_disequilibrium_(LD)#cite_note-3).

Genetic correlation analysis

To strengthen the understanding of the relationships between complex traits, we performed a genetic correlation analysis before MR analysis[72,73]. We first screened the evidence of genetic correlation between IDPs and psychiatric disorders using the LD score regression (https://github.com/bulik/ldsc)[74]. We used the default parameters of the software. Genetic correlation estimates were calculated using HapMap3 variants without the major histocompatibility complex regions suggested by the manual (https://alkesgroup.broadinstitute.org/LDSCORE/w_hm3.snplist.bz2). Precalculated LD scores were derived from the 1000 Genome European reference panel (https://data.broadinstitute.org/alkesgroup/LDSCORE/eur_w_ld_chr.tar.bz2). We used genetic correlation analysis to select IDPs potentially associated with psychiatric disorders for subsequent MR analysis. Therefore, the significant threshold for genetic correlation analysis was set as $P < 0.05$ to preserve all datasets with suggestive evidence.

MR analysis

Genetic instrument selection. We selected independent SNPs from GWAS summary data of exposure by using the clump function in PLINK 1.9 software (https://www.cog-genomics.org/plink/1.9/)[75]. The genomes of 315,147 Europeans from the UK Biobank were used as an LD reference. We constructed this reference data by sampling unrelated European ancestry individuals based on the genetic kinship information (Data-Field 22021), ethnic background information (Data-Field 21000) and genetic ethnic grouping information (Data-Field 22006) available from the UK Biobank (https://biobank.ndph.ox.ac.uk/). We also removed samples with sex chromosome aneuploidy (Data-Field 22019) and outliers for heterozygosity or missing rate (Data-Field 22027). We set an LD pruning r^2 threshold of 0.001, a window size of 1 Mb and a P value threshold of 5×10^{-8}. The selection of IVs should satisfy three assumptions: SNPs are strongly associated with exposure but not with outcome and not with confounding factors. SNPs with indirect LD effects ($r^2 > 0.8$) were also removed if they were associated with the outcome.

Removing confounders. We removed SNPs associated with confounders that interfere with the pathway between brain structures and psychiatric disorders. We considered four potential confounders, including socioeconomic status, education, drinking and smoking behavior. These traits have been reported by previous studies to influence both psychiatric disorders[76–78] and alterations of brain structure[79–81]. We used the PhenoScanner V2 database[82] (http://www.phenoscanner.medschl.cam.ac.uk/) and the NHGRI-EBI GWAS catalog[83] (https://www.ebi.ac.uk/gwas/docs/file-downloads/) to remove SNPs that were significantly associated with confounders in European participants. In addition, we also referred to the latest GWAS summary statistics on educational attainment[84], Townsend deprivation index at recruitment[85], average total household income before tax[85], alcohol dependence[86] and smoking behavior[87]. Finally, 139 confounder SNPs were removed (Supplementary Tables 4 and 5).

Quality control of IVs. To improve the accuracy and robustness of the genetic instruments, we proposed heterogeneity tests to detect outliers and adjusted them. We used Cochran's Q test for IVW model fitting in the case of horizontal pleiotropy effects[88] and Rucker's Q' test for MR-Egger model fitting in the case of directional pleiotropy effects[89]. We exploited the 'ivw_radial(alpha = 0.05, weights = 1,

tol = 0.0001)' and 'egger_radial(alpha = 0.05, weights = 1)' functions in the RadialMR v0.4R package (https://github.com/WSpiller/RadialMR/)[90] to calculate the modified Q and Q' test, respectively, and discarded the outliers with a nominal significance level of 0.05. Furthermore, we performed F-statistics to measure the power of IVs, with a threshold below 10 implying greater bias[91]. Briefly, the parameters required to test the F-statistics were R^2 (explained variance of genetic instruments on exposure), n (the sample size of GWAS for exposure) and k (the number of instruments).

$$F = \frac{R^2 \times (n-k-1)}{(1-R^2) \times k}$$

With summary statistics, we estimated the explained proportion of phenotypic variance of exposure by all SNPs served as instruments. The explained variance of IVs to exposure is actually the square of the correlation coefficient (R^2) between genetic variants and exposure. The parameters required to calculate the R^2 are β (genetic effect size from the exposure GWAS data) and s.e. (standard error of effect size). The formula for computing R^2 by a single instrumental variant is

$$R^2 = \frac{\beta^2}{\beta^2 + \text{s.e.}^2 \times n}.$$

The R^2 of multiple genetic variants is the sum of R^2 of each genetic variant.

Two-sample MR analyses. We performed two-sample MR analyses to explore the causal relationships between brain IDPs and psychiatric disorders. An IVW regression with a multiplicative random effects model was conducted as the primary causal inference[92]. IVW results may be biased when any of the SNPs has horizontal pleiotropy. We thus conducted four other MR methods to complement and enhance the reliability of the results. MR-RAPS accounts for systematic and idiosyncratic pleiotropy and can provide a robust inference for MR analysis with many weak instruments[93]. The MR-Egger method estimates the causal effect through the slope coefficient of the Egger regression, which provides a more robust estimate even if none of the IVs are invalid[94]. The weighted median method can even protect against up to 50% of invalid IVs[95]. The weighted mode method provides consistent estimates when the relaxed IV assumption has less bias and a lower type I error rate[29]. When only one genetic instrument was available, we used the Wald ratio[96] for MR analysis. All these methods were implemented by the functions 'mr_ivw', 'mr_raps', 'mr_weighted_median', 'mr_egger_regression', 'mr_weighted_mode' and 'mr_wald_ratio' in the TwoSampleMR v0.4.26 R package[69].

Sensitivity analysis. We verified the significant MR results after correction by sensitivity analysis. First, we performed leave-one-out analysis to check whether the causal association was obviously driven by a single SNP (a P value of <0.05 was regarded as an outlier). Second, we conducted MR-PRESSO (https://github.com/rondolab/MR-PRESSO/) to detect the presence of horizontal pleiotropy ($P < 0.05$)[97]. Third, we executed an MR-Egger regression to examine the potential bias of directional pleiotropy[94]. The intercept in the Egger regression indicates the mean pleiotropic effect of all genetic variants, which is interpreted as evidence of pleiotropy when the value differs from zero ($P < 0.05$).

Bidirectional MR. We extended the above MR analysis to a bidirectional causal inference between IDPs and psychiatric disorders. Forward MR analyses were performed with brain IDPs as exposures and psychiatric disorders as outcomes. Conversely, reverse MR analyses were performed with psychiatric disorders as exposures and brain IDPs as outcomes. For phenotypes that are highly polygenic (for example, schizophrenia identified 270 risk-associated loci[49]), challenges of horizontal pleiotropy are more likely to happen for MR[97,98]. We thus restricted the GWAS imputation score to ≥0.9 for genetic instruments. We performed MR analyses in accordance with the STROBE-MR checklist[99] and Burgess et al.'s guidelines[100].

Statistical power calculation

According to the method proposed by Burgess[24], we calculated the statistical power based on the sample size for each MR test. The parameters required to test the power of the hypothesis are R^2 (explained variance of genetic instruments on exposure), n (the sample size of outcome), ρ (the case–control ratio of outcome), β (estimated causal effect size per standard deviation change in exposure (in absolute terms)) and α (we set the significance levels at 0.05 and 4.49×10^{-5}). The formula for the power statistic in a binary outcome is

$$x = \left(n \times R^2 \times \left(\frac{\rho}{1+\rho}\right) \times \left(\frac{1}{1+\rho}\right)\right)^{\frac{1}{2}} \times \beta - f\left(1-\frac{\alpha}{2}\right).$$

The formula for the power statistic in a continuous outcome is

$$x = (n \times R^2)^{\frac{1}{2}} \times \beta - f\left(1-\frac{\alpha}{2}\right),$$

where, $f(x)$ denotes the quantile function of Gaussian distribution (also known as inverse cumulative distribution function). $F(x)$ denotes the cumulative distribution function.

$$F(x) = \int_{-\infty}^{x} \mathcal{N}(x|\mu, \sigma)$$

In our study, we calculated the OR (β) for each MR test at 80% power, with a significance level of 0.05. Multiple comparisons with a 4.49×10^{-5} error rate were also considered.

Test–retest correlation

Two different measures of IDP were used to evaluate the test–retest reliability. An initial measure of imaging data from the UK Biobank was in 2014, followed by the first repeat imaging visit in 2019. We selected brain IDP data from the same participant at both recording time points (test scan in 2014 and retest scan in 2019). A sample Pearson correlation coefficient was calculated between test and retest data, and the statistical power was determined using a two-sided t-test. Supplementary Table 1 provides the UK Biobank datafield ID for the individual-level phenotypic IDP data.

Standard deviation calculation of IDP

The reported OR is per standard deviation (1 s.d.) change in the mean of IDP. The standard deviation of each IDP was calculated based on the individual-level phenotypic data from the UK Biobank. Phenotypic measurements for these IDPs were selected from recording time points (2014 and 2019). The calculation was mainly based on the latest data collected in 2019. When the data in 2019 were unavailable, the data in 2014 were used. We used the R function 'sd()' to calculate standard deviation. The results are shown in Supplementary Table 1.

Reporting summary

Further information on research design is available in the Nature Research Reporting Summary linked to this article.

Data availability

All GWAS data are publicly available with the exception of the post-traumatic stress disorder data from Gelernter et al.[67]. These data are available through dbGaP accession number phs001672.v1.p1. Major depressive disorder GWAS data without the UK Biobank data were obtained by contacting the Psychiatric Genomics Consortium

workgroup data access committee representative (https://www.med.unc.edu/pgc/pgc-workgroups/major-depressive-disorder/). The GWASs for other psychiatric disorders were provided by the Psychiatric Genomics Consortium (https://www.med.unc.edu/pgc). Download links for all public datasets are available in Supplementary Table 2. The GWASs for brain IDPs can be obtained from the BIG40 web browser (https://open.win.ox.ac.uk/ukbiobank/big40/). Data in the NHGRI-EBI GWAS Catalog (v1.0.2-associtions_e104, released on 22 October 2021) were downloaded from https://www.ebi.ac.uk/gwas/docs/file-downloads/. Our results in the study are presented in our online platform at http://www.bigc.online/BrainMR/.

Code availability

The actual code used to run the analyses described in this study is available at our online platform (http://www.bigc.online/BrainMR/Browse/1.2-Code.html). All software packages we used in the study are publicly available, and the download links are included in the Methods.

References

60. Alfaro-Almagro, F. et al. Image processing and quality control for the first 10,000 brain imaging datasets from UK Biobank. *NeuroImage* **166**, 400–424 (2018).
61. Demontis, D. et al. Discovery of the first genome-wide significant risk loci for attention deficit/hyperactivity disorder. *Nat. Genet.* **51**, 63–75 (2019).
62. Otowa, T. et al. Meta-analysis of genome-wide association studies of anxiety disorders. *Mol. Psychiatry* **21**, 1391–1399 (2016).
63. Grove, J. et al. Identification of common genetic risk variants for autism spectrum disorder. *Nat. Genet.* **51**, 431–444 (2019).
64. Stahl, E. A. et al. Genome-wide association study identifies 30 loci associated with bipolar disorder. *Nat. Genet.* **51**, 793–803 (2019).
65. Wray, N. R. et al. Genome-wide association analyses identify 44 risk variants and refine the genetic architecture of major depression. *Nat. Genet.* **50**, 668–681 (2018).
66. International Obsessive Compulsive Disorder Foundation Genetics Collaborative (IOCDF-GC) and OCD Collaborative Genetics Association Studies (OCGAS). Revealing the complex genetic architecture of obsessive-compulsive disorder using meta-analysis. *Mol. Psychiatry* **23**, 1181–1188 (2018).
67. Gelernter, J. et al. Genome-wide association study of post-traumatic stress disorder reexperiencing symptoms in >165,000 US veterans. *Nat. Neurosci.* **22**, 1394–1401 (2019).
68. Yu, D. et al. Interrogating the genetic determinants of Tourette's syndrome and other tic disorders through genome-wide association studies. *Am. J. Psychiatry* **176**, 217–227 (2019).
69. Hemani, G. et al. The MR-Base platform supports systematic causal inference across the human phenome. *eLife* **7**, e34408 (2018).
70. Hartwig, F. P., Davies, N. M., Hemani, G. & Davey Smith, G. Two-sample Mendelian randomization: avoiding the downsides of a powerful, widely applicable but potentially fallible technique. *Int. J. Epidemiol.* **45**, 1717–1726 (2016).
71. Price, A. L. et al. Long-range LD can confound genome scans in admixed populations. *Am. J. Hum. Genet.* **83**, 132–135 (2008). author reply 135-139.
72. Zheng, J. et al. Recent developments in Mendelian randomization studies. *Curr. Epidemiol. Rep.* **4**, 330–345 (2017).
73. Kraft, P., Chen, H. & Lindstrom, S. The use of genetic correlation and Mendelian randomization studies to increase our understanding of relationships between complex traits. *Curr. Epidemiol. Rep.* **7**, 104–112 (2020).
74. Bulik-Sullivan, B. et al. An atlas of genetic correlations across human diseases and traits. *Nat. Genet.* **47**, 1236–1241 (2015).
75. Purcell, S. et al. PLINK: a tool set for whole-genome association and population-based linkage analyses. *Am. J. Hum. Genet.* **81**, 559–575 (2007).
76. McLaughlin, K. A., Costello, E. J., Leblanc, W., Sampson, N. A. & Kessler, R. C. Socioeconomic status and adolescent mental disorders. *Am. J. Public Health* **102**, 1742–1750 (2012).
77. Hjorthoj, C. et al. Association between alcohol and substance use disorders and all-cause and cause-specific mortality in schizophrenia, bipolar disorder, and unipolar depression: a nationwide, prospective, register-based study. *Lancet Psychiatry* **2**, 801–808 (2015).
78. Gurillo, P., Jauhar, S., Murray, R. M. & MacCabe, J. H. Does tobacco use cause psychosis? Systematic review and meta-analysis. *Lancet Psychiatry* **2**, 718–725 (2015).
79. Noble, K. G. et al. Family income, parental education and brain structure in children and adolescents. *Nat. Neurosci.* **18**, 773–778 (2015).
80. Li, L. et al. Lower regional grey matter in alcohol use disorders: evidence from a voxel-based meta-analysis. *BMC Psychiatry* **21**, 247 (2021).
81. Schneider, C. E. et al. Smoking status as a potential confounder in the study of brain structure in schizophrenia. *J. Psychiatr. Res.* **50**, 84–91 (2014).
82. Kamat, M. A. et al. PhenoScanner V2: an expanded tool for searching human genotype-phenotype associations. *Bioinformatics* **35**, 4851–4853 (2019).
83. Buniello, A. et al. The NHGRI-EBI GWAS catalog of published genome-wide association studies, targeted arrays and summary statistics 2019. *Nucleic Acids Res.* **47**, D1005–D1012 (2019).
84. Lee, J. J. et al. Gene discovery and polygenic prediction from a genome-wide association study of educational attainment in 1.1 million individuals. *Nat. Genet.* **50**, 1112–1121 (2018).
85. Jiang, L. et al. A resource-efficient tool for mixed model association analysis of large-scale data. *Nat. Genet.* **51**, 1749–1755 (2019).
86. Walters, R. K. et al. Transancestral GWAS of alcohol dependence reveals common genetic underpinnings with psychiatric disorders. *Nat. Neurosci.* **21**, 1656–1669 (2018).
87. Tobacco and Genetics Consortium. Genome-wide meta-analyses identify multiple loci associated with smoking behavior. *Nat. Genet.* **42**, 441–447 (2010).
88. Greco, M. F., Minelli, C., Sheehan, N. A. & Thompson, J. R. Detecting pleiotropy in Mendelian randomisation studies with summary data and a continuous outcome. *Stat. Med.* **34**, 2926–2940 (2015).
89. Rucker, G., Schwarzer, G., Carpenter, J. R., Binder, H. & Schumacher, M. Treatment-effect estimates adjusted for small-study effects via a limit meta-analysis. *Biostatistics* **12**, 122–142 (2011).
90. Bowden, J. et al. Improving the visualization, interpretation and analysis of two-sample summary data Mendelian randomization via the radial plot and radial regression. *Int. J. Epidemiol.* **47**, 2100 (2018).
91. Burgess, S., Thompson, S. G. & CRP CHD Genetics Collaboration. Avoiding bias from weak instruments in Mendelian randomization studies. *Int. J. Epidemiol.* **40**, 755–764 (2011).
92. Burgess, S., Butterworth, A. & Thompson, S. G. Mendelian randomization analysis with multiple genetic variants using summarized data. *Genet. Epidemiol.* **37**, 658–665 (2013).
93. Zhao, Q. Y., Wang, J. S., Hemani, G., Bowden, J. & Small, D. S. Statistical inference in two-sample summary-data Mendelian randomization using robust adjusted profile score. *Ann. Stat.* **48**, 1742–1769 (2020).
94. Bowden, J., Davey Smith, G. & Burgess, S. Mendelian randomization with invalid instruments: effect estimation and bias detection through Egger regression. *Int. J. Epidemiol.* **44**, 512–525 (2015).

95. Bowden, J., Davey Smith, G., Haycock, P. C. & Burgess, S. Consistent estimation in Mendelian randomization with some invalid instruments using a weighted median estimator. *Genet. Epidemiol.* **40**, 304–314 (2016).
96. Wald, A. The fitting of straight lines if both variables are subject to error. *Ann. Math. Stat.* **11**, 284–300 (1940).
97. Verbanck, M., Chen, C. Y., Neale, B. & Do, R. Detection of widespread horizontal pleiotropy in causal relationships inferred from Mendelian randomization between complex traits and diseases. *Nat. Genet.* **50**, 693–698 (2018).
98. VanderWeele, T. J., Tchetgen Tchetgen, E. J., Cornelis, M. & Kraft, P. Methodological challenges in Mendelian randomization. *Epidemiology* **25**, 427–435 (2014).
99. Skrivankova, V. W. et al. Strengthening the reporting of observational studies in epidemiology using Mendelian randomization: the STROBE-MR statement. *JAMA* **326**, 1614–1621 (2021).
100. Burgess, S. et al. Guidelines for performing Mendelian randomization investigations. *Wellcome Open Res* **4**, 186 (2019).

Acknowledgements

This work was supported by grants from the National Natural Science Foundation of China (grant numbers 32170616 (T.-L.Y.), 82170896 (Y.G.), 31970569 (Y.G.) and 82101601 (S.Y.)), Science Fund for Distinguished Young Scholars of Shaanxi Province (grant number 2021JC-02 (T.-L.Y.)), Innovation Capability Support Program of Shaanxi Province (grant number 2022TD-44 (T.-L.Y.)) and the Fundamental Research Funds for the Central Universities (T.-L.Y.). This work was also supported by the High-Performance Computing Platform and Instrument Analysis Center of Xi'an Jiaotong University. We would like to thank the UK Biobank and Cross-Disorder Group of the Psychiatric Genomics Consortium for the GWAS summary data of IDPs and psychiatric disorders. We also thank the US Million Veteran Program and dbGaP. The GWAS summary data of posttraumatic stress disorder that we used are available from the dbGaP database under dbGaP accession number phs001672.v1.p1. We thank the UK Biobank Resource under application number 46387.

Author contributions

J.G. conducted this project and wrote the manuscript. K.Y. built the database website and drew the figures. S.-S.D. and Y.G. revised the manuscript. S.Y. applied for the UK Biobank data and offered some advice. Y.R. and H.W. drew the figures and collected materials for the online database. K.Z. and F.J. summarized the UK Biobank data. Y.-X.C. applied for the dbGaP data. T.-L.Y. and Y.G. conceived and supervised this project.

Competing interests

The authors declare no competing interests.

Additional information

Supplementary information The online version contains supplementary material available at https://doi.org/10.1038/s41593-022-01174-7.

Correspondence and requests for materials should be addressed to Yan Guo or Tie-Lin Yang.

Peer review information *Nature Neuroscience* thanks Baptiste Couvy-Duchesne, Miguel Renteria, and the other, anonymous reviewer(s) for their contribution to the peer review of this work.

nature portfolio

Corresponding author(s): Tie-Lin Yang, Yan Guo

Last updated by author(s): Aug 22, 2022

Reporting Summary

Nature Portfolio wishes to improve the reproducibility of the work that we publish. This form provides structure for consistency and transparency in reporting. For further information on Nature Portfolio policies, see our Editorial Policies and the Editorial Policy Checklist.

Statistics

For all statistical analyses, confirm that the following items are present in the figure legend, table legend, main text, or Methods section.

n/a	Confirmed	
☐	☒	The exact sample size (*n*) for each experimental group/condition, given as a discrete number and unit of measurement
☒	☐	A statement on whether measurements were taken from distinct samples or whether the same sample was measured repeatedly
☐	☒	The statistical test(s) used AND whether they are one- or two-sided *Only common tests should be described solely by name; describe more complex techniques in the Methods section.*
☒	☐	A description of all covariates tested
☐	☒	A description of any assumptions or corrections, such as tests of normality and adjustment for multiple comparisons
☐	☒	A full description of the statistical parameters including central tendency (e.g. means) or other basic estimates (e.g. regression coefficient) AND variation (e.g. standard deviation) or associated estimates of uncertainty (e.g. confidence intervals)
☐	☒	For null hypothesis testing, the test statistic (e.g. *F*, *t*, *r*) with confidence intervals, effect sizes, degrees of freedom and *P* value noted *Give P values as exact values whenever suitable.*
☒	☐	For Bayesian analysis, information on the choice of priors and Markov chain Monte Carlo settings
☒	☐	For hierarchical and complex designs, identification of the appropriate level for tests and full reporting of outcomes
☐	☒	Estimates of effect sizes (e.g. Cohen's *d*, Pearson's *r*), indicating how they were calculated

Our web collection on statistics for biologists contains articles on many of the points above.

Software and code

Policy information about availability of computer code

Data collection	No software was used for data collection.
Data analysis	The following software packages were used in this work: LD-based result clumping was performed using PLINK 1.9 (https://www.cog-genomics.org/plink/1.9/). Genetic correlation analysis was performed using LDSC software v1.0.0 (https://github.com/bulik/ldsc). R version 3.3.2 (https://www.r-project.org/) was used for statistical analysis. The TwoSampleMR v0.4.26 R package (https://mrcieu.github.io/TwoSampleMR/), RadialMR v0.4 (https://github.com/WSpiller/RadialMR/) and MR-PRESSO v1.0 (https://github.com/rondolab/MR-PRESSO/) were used for MR analyses. PhenoScanner V2 GWAS database (http://www.phenoscanner.medschl.cam.ac.uk/) was used to remove confounding factors. The brain templates in diagrams were from BrainNet software v1.7 (https://www.nitrc.org/projects/bnv). The custom code used to run the these software is available at our online platform (http://www.bigc.online/BrainMR/Browse/1.2-Code.html).

For manuscripts utilizing custom algorithms or software that are central to the research but not yet described in published literature, software must be made available to editors and reviewers. We strongly encourage code deposition in a community repository (e.g. GitHub). See the Nature Portfolio guidelines for submitting code & software for further information.

Data

Policy information about availability of data

All manuscripts must include a data availability statement. This statement should provide the following information, where applicable:

- Accession codes, unique identifiers, or web links for publicly available datasets
- A description of any restrictions on data availability
- For clinical datasets or third party data, please ensure that the statement adheres to our policy

GWAS statistics of brain IDPs were collected from BIG40 web browser (https://open.win.ox.ac.uk/ukbiobank/big40/). GWAS statistics of attention deficit hyperactivity disorder (https://figshare.com/ndownloader/files/28169253/daner_adhd_meta_filtered_NA_iPSYCH23_PGC11_sigPCs_woSEX_2ell6sd_EUR_Neff_70.meta.gz), anorexia nervosa (https://figshare.com/ndownloader/files/28169271/pgcAN2.2019-07.vcf.tsv.gz), anxiety (https://figshare.com/ndownloader/files/28570812/anxiety.meta.full.cc.tbl.gz), autism spectrum disorder (https://figshare.com/ndownloader/files/28169292/iPSYCH-PGC_ASD_Nov2017.gz), bipolar disorder (https://figshare.com/ndownloader/files/28169307/daner_PGC_BIP32b_mds7a_0416a.gz), major depressive disorder GWAS data without UK Biobank were obtained by contacting the Psychiatric Genomics Consortium workgroup data access committee representative (https://www.med.unc.edu/pgc/pgc-workgroups/major-depressive-disorder/). obsessive-compulsive disorder (https://figshare.com/ndownloader/files/28169544/ocd_aug2017.gz), schizophrenia (https://figshare.com/ndownloader/files/34517807/PGC3_SCZ_wave3.core.autosome.public.v3.vcf.tsv), Tourette syndrome (https://figshare.com/ndownloader/files/28169940/TS_Oct2018.gz), post-traumatic stress disorder were collected from the US Million Veteran Program, and available via dbGaP (phs001672.v1.p1) (https://www.ncbi.nlm.nih.gov/projects/gap/cgi-bin/study.cgi?study_id=phs001672.v1.p1). GWAS statistics of other traits, educational attainment is from social science genetic association consortium (SSGAC) (https://www.thessgac.org). Alcohol dependence (unrelated individuals of European ancestry) and smoking behavior (ever vs never smoked) were all collected from Psychiatric Genomics Consortium (https://www.med.unc.edu/pgc/download-results). Townsend deprivation index at recruitment and average total household income before tax are from fastGWA data portal (https://yanglab.westlake.edu.cn/data/ukb_fastgwa/imp/). Genomes references were constructed by applying genotype data from the UK Biobank (https://biobank.ndph.ox.ac.uk/). Data in the NHGRI-EBI GWAS Catalog (v1.0.2-associtions_e105, release in 22 October 2021) were downloaded from https://www.ebi.ac.uk/gwas/docs/file-downloads/.

Human research participants

Policy information about studies involving human research participants and Sex and Gender in Research.

Reporting on sex and gender	We used the public data, and the participants were the same as the original data and vary from dataset to dataset. Detailed sample information can be accessed in the references, for example, IDP (Smith et al., 2021), ADHD (Demontis et al., 2019), AN (Watson et al., 2019), ANX (Otowa et al., 2016), ASD (Grove et al., 2019), BD (Stahl et al., 2019), MDD (Wray et al., 2018), OCD (IOCDF-GC and OCGAS, 2018), PTSD (Gelernter et al., 2019), SCZ (Trubetskoy et al., 2022) and TS (Yu et al., 2019). Briefly, sex differences were not significant in the data for the other phenotypes, except for PTSD, which was predominantly male in the sample, accounting for approximately 93.3% of the total sample.
Population characteristics	We used the public data, and the participants were the same as the original data and vary from dataset to dataset. Detailed sample information can be accessed in the references. Analyses were conducted on GWAS summary statistics for 587 IDPs with a sample size of up to 33,224 subjects of European ancestry. We collected 10 psychiatric disorders with publicly available GWAS summary statistics, including attention deficit hyperactivity disorder (ADHD), anorexia nervosa, autism spectrum disorder, bipolar disorder, major depressive disorder, obsessive-compulsive disorder, post-traumatic stress disorder (PTSD), schizophrenia, tourette syndrome and anxiety. Most of these data were derived from Psychiatric Genomics Consortium (PGC), except for PTSD symptoms in the US Million Veteran Program (MVP). The sample sizes for these 10 disorders ranged from 9,725 to 161,405 subjects. Full description of sample characteristics of each study are provided in Supplementary Tables 1 and 2.
Recruitment	We used the public data, and the participants were the same as the original data and vary from dataset to dataset. Detailed sample information can be accessed in the references.
Ethics oversight	The GWAS summary data we used are all publicly released, and ethical approval was provided in each study.

Note that full information on the approval of the study protocol must also be provided in the manuscript.

Field-specific reporting

Please select the one below that is the best fit for your research. If you are not sure, read the appropriate sections before making your selection.

☒ Life sciences ☐ Behavioural & social sciences ☐ Ecological, evolutionary & environmental sciences

For a reference copy of the document with all sections, see nature.com/documents/nr-reporting-summary-flat.pdf

Life sciences study design

All studies must disclose on these points even when the disclosure is negative.

Sample size	To enhance study power, the largest available genome-wide association studies were used for both exposure and outcome measures to carry

Sample size	out Mendelian randomization. The sample size for 587 IDPs (N = ~33,224) are summarized in Supplementary Table 1. The sample size for 10 psychiatric (N = 9,725 to 161,405) are summarized in Supplementary Table 2. We calculated the statistical power for each MR test based on the sample size, and the results summarized in Supplementary Tables 8-9.
Data exclusions	No data were excluded.
Replication	No other cohort of this magnitude available for replication at this stage.
Randomization	Not relevant; no experimental procedures were performed as this was a study of Mendel randomization (MR). MR is an epidemiological method that uses genetic variants as instrument to infer the causality between exposure factors and outcomes.
Blinding	Not relevant; there were no experimental groups.

Reporting for specific materials, systems and methods

We require information from authors about some types of materials, experimental systems and methods used in many studies. Here, indicate whether each material, system or method listed is relevant to your study. If you are not sure if a list item applies to your research, read the appropriate section before selecting a response.

Materials & experimental systems

n/a	Involved in the study
☒	☐ Antibodies
☒	☐ Eukaryotic cell lines
☒	☐ Palaeontology and archaeology
☒	☐ Animals and other organisms
☒	☐ Clinical data
☒	☐ Dual use research of concern

Methods

n/a	Involved in the study
☒	☐ ChIP-seq
☒	☐ Flow cytometry
☐	☒ MRI-based neuroimaging

Magnetic resonance imaging

Experimental design

Design type	Our analyses include data from structural MRI and diffusion MRI. Please see "Methods" for full details. The information of brain MRI is provided by UK Biobank online refs (https://biobank.ctsu.ox.ac.uk/crystal/crystal/docs/brain_mri.pdf) (Alfaro-Almagro, NeuroImage 2018).
Design specifications	MRI data processing (to generate imaging-derived phenotypes) was done previously and is full described in the references (Alfaro-Almagro, NeuroImage (2018); Smith et al., Nature Neuroscience (2021); Miller et al., Nature Neuroscience (2016) and Elliott et al., Nature (2018)).
Behavioral performance measures	Behavioral performance in the MRI scanner was not used in this study.

Acquisition

Imaging type(s)	Please see "Methods" and Supplementary Table 1 for full details. Our analyses include data from Structural MRI and diffusion MRI.
Field strength	3T
Sequence & imaging parameters	MRI data processing (to generate imaging-derived phenotypes) was done previously and is full described in the references (Alfaro-Almagro, NeuroImage (2018); Smith et al., Nature Neuroscience (2021); Miller et al., Nature Neuroscience (2016) and Elliott et al., Nature (2018)).
Area of acquisition	Siemens' auto-align was used to include the full brain in the imaged field-of-view; this was checked (and corrected if necessary) by the radiographer.

Diffusion MRI ☒ Used ☐ Not used

Parameters: Please see above for information about full details.

Preprocessing

Preprocessing software	See above (covered previously in full detail in references of Alfaro-Almagro, NeuroImage (2018); Smith et al., Nature Neuroscience (2021); Miller et al., Nature Neuroscience (2016) and Elliott et al., Nature (2018).)
Normalization	See above (covered previously in full detail in references of Alfaro-Almagro, NeuroImage (2018); Smith et al., Nature

Normalization	Neuroscience (2021); Miller et al., Nature Neuroscience (2016) and Elliott et al., Nature (2018).)
Normalization template	See above (covered previously in full detail in references of Alfaro-Almagro, NeuroImage (2018); Smith et al., Nature Neuroscience (2021); Miller et al., Nature Neuroscience (2016) and Elliott et al., Nature (2018).)
Noise and artifact removal	See above (covered previously in full detail in references of Alfaro-Almagro, NeuroImage (2018); Smith et al., Nature Neuroscience (2021); Miller et al., Nature Neuroscience (2016) and Elliott et al., Nature (2018).)
Volume censoring	See above (covered previously in full detail in references of Alfaro-Almagro, NeuroImage (2018); Smith et al., Nature Neuroscience (2021); Miller et al., Nature Neuroscience (2016) and Elliott et al., Nature (2018).)

Statistical modeling & inference

Model type and settings	See above (covered previously in full detail in references of Alfaro-Almagro, NeuroImage (2018); Smith et al., Nature Neuroscience (2021); Miller et al., Nature Neuroscience (2016) and Elliott et al., Nature (2018).)
Effect(s) tested	See above (covered previously in full detail in references of Alfaro-Almagro, NeuroImage (2018); Smith et al., Nature Neuroscience (2021); Miller et al., Nature Neuroscience (2016) and Elliott et al., Nature (2018).)

Specify type of analysis: ☐ Whole brain ☐ ROI-based ☒ Both

Anatomical location(s)	Based on the reliable segmentation and meaningful measurement, 587 brain structural IDPs were selected from the 3,913 original releases, including 203 IDPs in cerebral cortex, 24 IDPs in subcortical regions, and 360 IDPs of white matter connections. We further classified these IDPs into 13 regional categories and 9 measures (see Figure 1). Details of these neuroimaging measures and processing methods are provided by the online reference of UK Biobank (https://biobank.ctsu.ox.ac.uk/crystal/crystal/docs/brain_mri.pdf).
Statistic type for inference (See Eklund et al. 2016)	Statisctis for inference was not carried out when generating IDPs, but within this study inference was applied at the level of the combined imaging-genetics modelling. We conducted a Mendelian randomization study to explore the causality of brain imaging-derived phenotypes on 10 psychiatric disorders.
Correction	In this study, we performed sensitivity analyses to validate the causal effects on significant results. For the multiple testing correction, we used the Bonferroni correction for MR analyses ($p < 4.49E-5$).

Models & analysis

n/a	Involved in the study
☒	☐ Functional and/or effective connectivity
☒	☐ Graph analysis
☒	☐ Multivariate modeling or predictive analysis